6 Marshall Islands

6.1 Summary

6.1.1 Climate

- Changes in air temperature from season to season are relatively small, with air temperatures strongly linked to changes in the surrounding ocean temperature. The Republic of Marshall Islands (RMI) has a wet season from May to November and a dry season from December to April.
- The seasonal cycle of rainfall is affected by the Intertropical Convergence Zone (ITCZ). In some years, the West Pacific Monsoon (WPM) also affects rainfall.
- Annual and seasonal air temperatures at Majuro and Kwajalein have increased since the 1950s. The number of warm nights has increased, and the number of cool days and cold nights has decreased at both sites. The energy required for cooling indoor environments has also increased at both sites.
- The longest run of days without rain has been decreasing at Majuro. All other annual, seasonal and extreme rainfall trends show little change at Majuro and Kwajalein.
- Tropical cyclones affect Marshall Islands year-round. Over the period 1969–2017, an average of 23 cyclones passed within the RMI exclusive economic zone (EEZ) per decade. Tropical cyclones were most frequent in El Niño years and least frequent in La Niña years. Year-to-year variability is large, ranging from no tropical cyclones in some years to 11 in 1972 and 1997.
- There has been little change in the number of severe tropical cyclones or the total number of tropical cyclones in the Northwest Pacific since 1981.

6.1.2 Ocean

- Highest sea levels typically occur from September to March.
- Sea-level rise within the EEZ, measured by satellite altimeters since 1993, is about 1.0 to 4.5 mm (0.04 to 0.18 in) per year.
- Monthly average ocean temperature, measured by the Majuro tide-gauge, ranges from 28 °C (82.4 °F) in February to 29.5 °C (85.1 °F) in September/October. However, monthly temperatures in any given year can be ±2 °C (±3.6 °F) of these averages.
- The sea surface temperature (SST) trend in the EEZ is 0.25 °C (0.45 °F) per decade.
- Dominant wave direction is from 54° (NE), with an average significant wave height of 1.56 m (5.12 ft) and average wave period of 9.7 s.
- Severe wave height was defined as 3.09 m (10.14 ft), with an average of 2.6 severe events per year.
- Peak average significant wave height occurs from November to March.

6.2 Country description

Located in the equatorial/tropical North Pacific Ocean, RMI is made up of 29 atolls and five individual islands between latitudes 3°N and 15°N, and longitudes 161°E and 173°E (Figure 6.1). The atolls and islands form two parallel chains running northwest to southeast: Ratak (sunrise) and Ralik (sunset). The largest atoll, with a land area of 16 km^2, is Kwajalein (Ralik chain). RMI has a total land area of 180 km^2 and an EEZ of 2.1 million km^2. The capital and largest city is Majuro, located on Majuro Atoll. The highest elevation is about 10 m (33 ft) above sea level on Likiep Atoll. RMI's population is approximately 59,100. About 52% of the population live on Majuro Atoll.

Figure 6.1:
Marshall Islands (RMI) and the locations of the climate stations used in this report

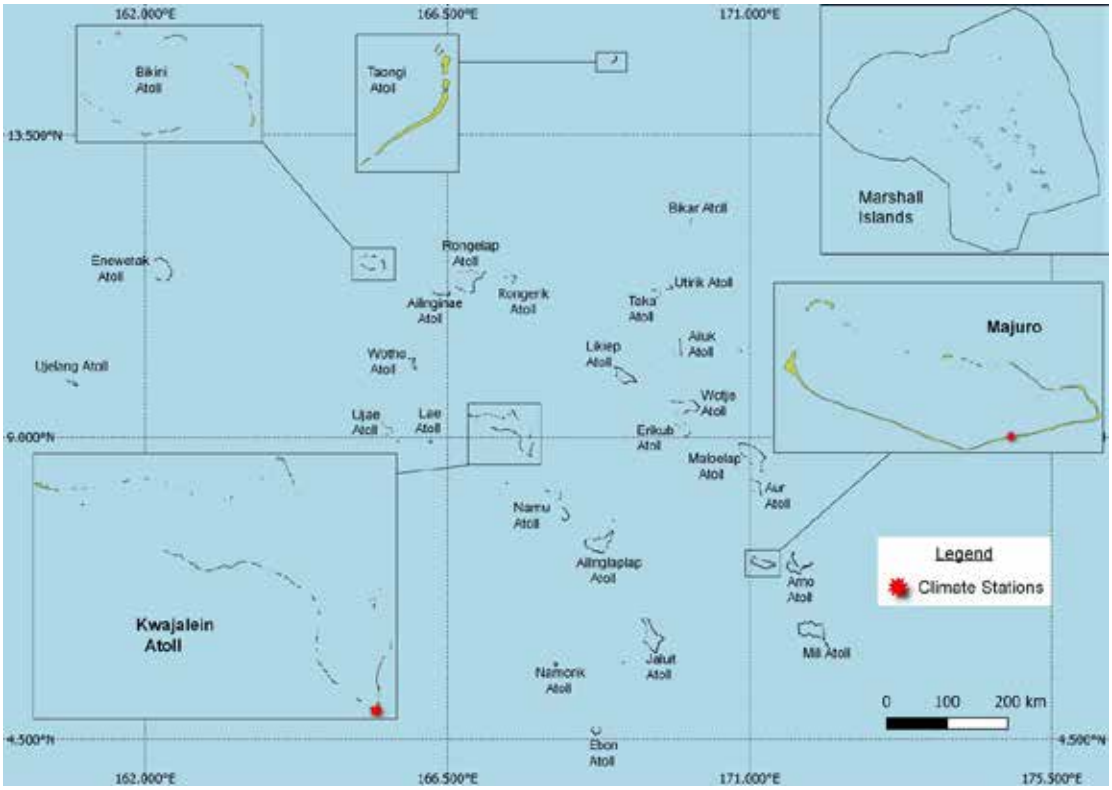

6.3 Data

Daily historical rainfall and air temperature records for Majuro and Kwajalein from 1951 were obtained from the United States National Oceanic and Atmospheric Administration Majuro Weather Service Office. These records have undergone data quality and homogeneity assessment. Where the maximum or minimum air temperature records were found to have discontinuities, these records have been adjusted to make them homogeneous (further information is provided in Chapter 1). Additional information on historical climate trends for RMI can be found in the Pacific Climate Change Data Portal http://www.bom.gov.au/climate/pccsp.

Tropical cyclone data and historical tracks starting from the 1969 season are available from the Western North Pacific Tropical Cyclone Data Portal http://www.bom.gov.au/cyclone/history/tracks/beta/?region=wnp.

SST covering the EEZ was obtained via the daily Optimum Interpolation SST version 2.1 (OISST v2.1) dataset from NOAA (Reynolds et al. 2007; Banzon et al. 2016). In situ ocean temperature data were obtained from the PSLGM Project tide-gauge located at Majuro, with data spanning from 1993 to 2021.

Wave data were obtained from the PACCSAP wave hindcast (Smith et al. 2021), available hourly from 1979 to 2021, with a grid resolution near RMI of 7 km (4.3 mi).

Regional sea level data were obtained from CSIRO satellite altimetry (updated by Benoit Legresy, Church and White 2011), with correction for seasonal signals, inverse barometer effect and glacial isostatic adjustment. Tide-gauge data were sourced from the Majuro tide-gauge station, spanning from 1993 to 2021 at hourly intervals.

6.4 Rainfall

6.4.1 Seasonal cycle

RMI is located in an area where the ITCZ produces high rainfall throughout the year (Figure 6.2). This band of heavy rainfall is caused by air rising over warm water where winds converge and is most intense and closest to RMI during the wet season months of May to November. Rainfall in some years is also influenced by the WPM, which brings wetter conditions when it is active over RMI.

Majuro receives 65% of the rainfall during the wet season, which averages 2197 mm (86.4 in) and 1187 mm (46.7 in) in the dry season. In Kwajalein, the average rainfall in the wet season is 1832 mm (71.2 in), which is 72% of the annual total. Kwajalein has a more distinct dry season, with the driest months (January–March) receiving about 100 mm (3.9 in) on average.

Figure 6.2:
Mean annual rainfall at Majuro and Kwajalein

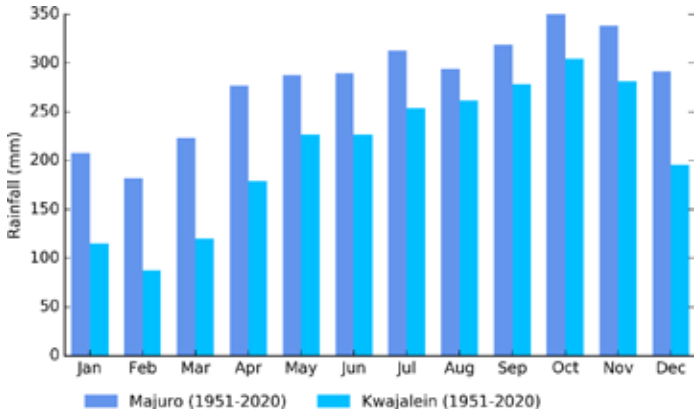

6.4.2 Trends

Trends in annual and seasonal rainfall are not statistically significant at Majuro and Kwajalein (Figure 6.3, Table 6.1). Annual and seasonal rainfall trends indicate little change at both sites.

Annual rainfall varies from approximately 2200 to 4500 mm (86.6 to 177.2 in) at Majuro and from approximately 1500 to 3700 mm (59.1 to 145.7 in) at Kwajalein. Approximately half of all days each year experience rain at Kwajalein and more than half of all days experience rain at Majuro (Figure 6.3).

Figure 6.3:
Annual rainfall (bar graph) and number of wet days (where rainfall is at least 1 mm, line graph) at Majuro (left) and Kwajalein (right). Straight lines indicate linear trends for annual rainfall (in black) and number of wet days (in blue). The magnitudes of the trends are presented in Table 6.1. Diamonds indicate years with insufficient data for one or both variables.

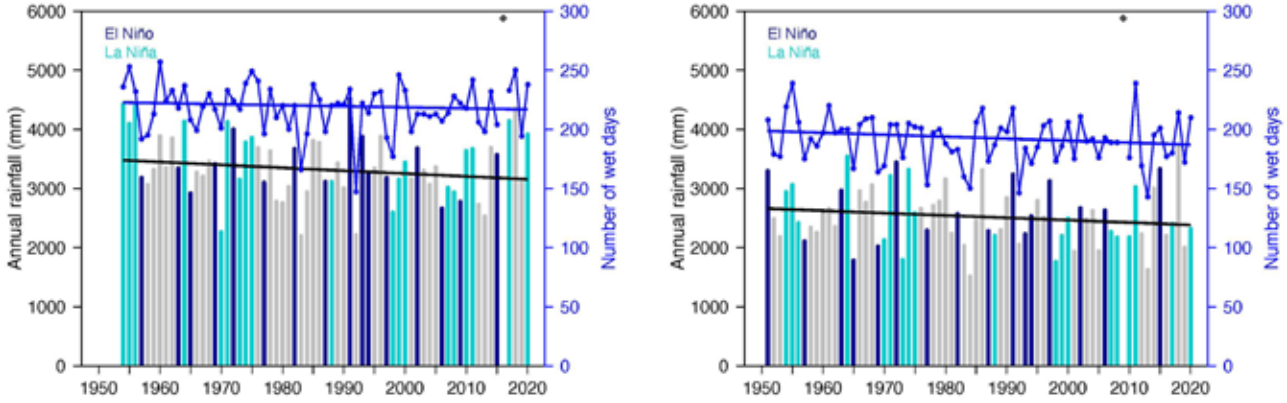

Table 6.1:
Trends in annual, seasonal and extreme rainfall at Majuro (left) and Kwajalein (right). The 95% confidence intervals are shown in parentheses, and trends significant at the 95% level are shown in bold. The contribution to total rainfall from extreme events and the standardised rainfall evapotranspiration index are measured relative to 1961–1990 (see Chapter 1 for details).

	Majuro	Kwajalein
	1954–2020	1951–2020
Annual rainfall (mm/decade)	-48.90 (-125.80, +16.97)	-39.95 (-99.17, +20.32)
November–April (mm/decade)	-5.76 (-64.37, +44.23)	+3.39 (-34.54, +41.16)
May–October (mm/decade)	-28.18 (-72.92, +23.73)	-29.88 (-65.78, +6.39)
Number of wet days (days/decade)	-0.91 (-3.66, +1.52)	-1.67 (-4.17, +0.93)
Contribution to total rainfall from extreme events (%/decade)	-0.79 (-1.75, +0.25)	+0.48 (-0.76, +1.66)
Consecutive dry days (days/decade)	**-0.48** (-0.91, 0.00)	0.00 (-0.57, +0.53)
Maximum one-day rainfall (mm/decade)	-0.97 (-6.33, +3.67)	+3.13 (-1.62, +7.88)
Standardised rainfall evapotranspiration index (November–April)	+0.01 (-0.15, +0.14)	+0.04 (-0.10, +0.18)
Standardised rainfall evapotranspiration index (May–October)	-0.08 (-0.24, +0.09)	-0.07 (-0.19, +0.05)

The longest run of days without rain each year has been decreasing at Majuro since 1954 (Figure 6.4). No significant trends in any other extreme rainfall indices were detected at either Majuro or Kwajalein (Table 6.1). An unusually high maximum daily rainfall at Majuro in 1972 was a result of tropical cyclone Violet.

Figure 6.4:
Annual longest run of consecutive dry days (bar graph) and maximum daily rainfall (line graph) at Majuro (left) and Kwajalein (right). Straight lines indicate linear trends for dry days (in black) and maximum daily rainfall (in blue). The magnitudes of the trends are presented in Table 6.1. Diamonds indicate years with insufficient data for one or both variables.

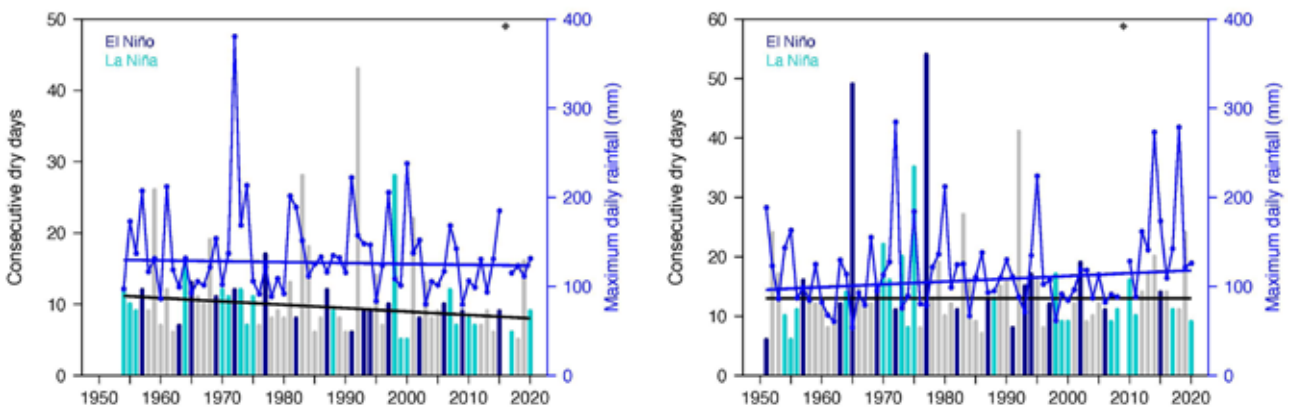

6.5 Air temperature

6.5.1 Seasonal cycle

The average air temperature across RMI is relatively constant year-round, with any changes in air temperatures strongly linked to changes in the surrounding ocean temperature (Figure 6.5). There has been a clear shift towards warmer average monthly temperatures between the climatology periods of 1961–1990 and 1991–2020, with warmer average temperatures occurring in all months throughout the year for both Majuro and Kwajalein, with the exception of average maximum temperatures at Kwajalein between October and April.

Figure 6.5:
Maximum and minimum air temperature seasonal cycle for Majuro (purple) and Kwajalein (green), and for the periods 1961–1990 (dotted lines) and 1991–2020 (solid lines)

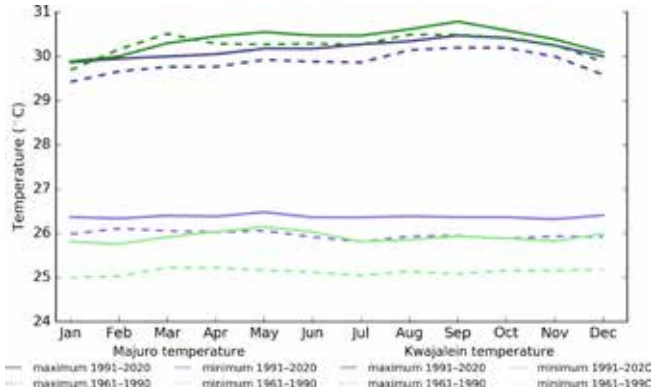

6.5.2 Trends

Average annual and seasonal temperatures have increased significantly at Majuro and Kwajalein (Figure 6.6, Table 6.2). Daily minimum temperatures are warming faster than daily maximum temperatures at Kwajalein. Variability consistent with the Interdecadal Pacific Oscillation is evident at Majuro, although this could be influenced by data quality issues in the mid-1970s.

Figure 6.6:
Annual, November–April and May–October average temperatures for Majuro (left) and Kwajalein (right). Straight lines indicate linear trends. The magnitudes of the trends are presented in Table 6.2. Diamonds indicate years with insufficient data for one or more variables.

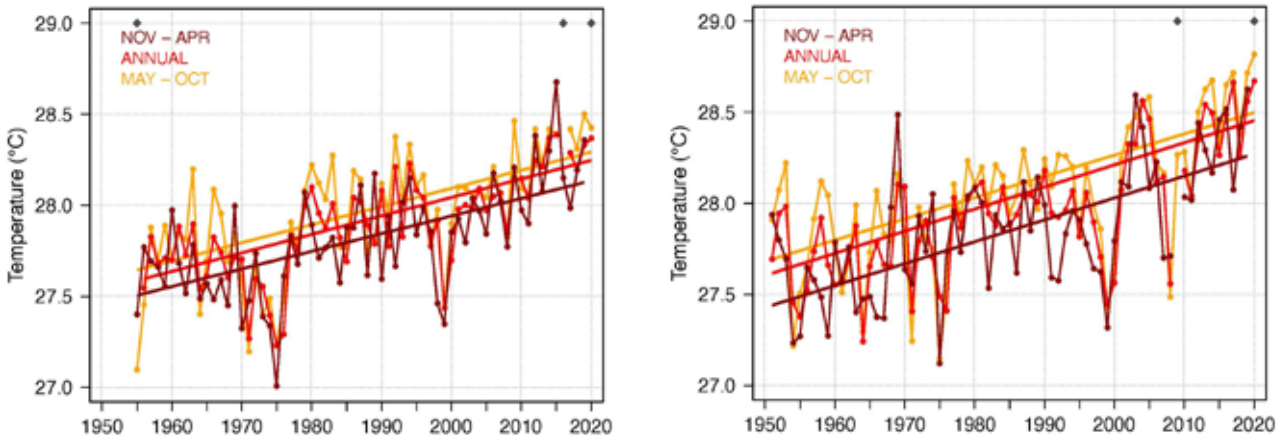

Table 6.2:
Trends in annual and seasonal air temperatures at Majuro (left) and Kwajalein (right). The 95% confidence intervals are shown in parentheses, and trends significant at the 95% level are shown in bold.

	Majuro Tmax (°C/decade)	Majuro Tmin (°C/decade)	Majuro Tmean (°C/decade)	Kwajalein Tmax (°C/10yrs)	Kwajalein Tmin (°C/10yrs)	Kwajalein Tmean (°C/10yrs)
	1955–2020			1951–2020		
Annual	**+0.09** (+0.02, +0.16)	**+0.12** (+0.08, +0.16)	**+0.10** (+0.07, +0.14)	**+0.09** (+0.01, +0.17)	**+0.14** (+0.08, +0.19)	**+0.12** (+0.08, +0.17)
November–April	**+0.10** (+0.04, +0.16)	**+0.10** (+0.07, +0.13)	**+0.10** (+0.06, +0.13)	**+0.11** (+0.03, +0.18)	**+0.14** (+0.09, +0.20)	**+0.12** (+0.08, +0.16)
May–October	+0.07 (0.00, +0.15)	**+0.12** (+0.09, +0.17)	**+0.10** (+0.05, +0.15)	**+0.09** (+0.01, +0.17)	**+0.14** (+0.10, +0.20)	**+0.12** (+0.08, +0.17)

The number of warm nights has increased at Majuro and Kwajalein, and the number of cool days and cold nights has decreased (Figure 6.7, Table 6.3). Decade-to-decade variability can be seen in the number of hot days at both sites.

The cooling degree days index provides a measure of the energy demand needed to cool a building down to 25 °C (77.0 °F), with the assumption that air conditioners are generally turned on at this temperature. There has been an increase in the cooling degree days index at both sites, suggesting the energy needed for cooling has increased significantly.

Table 6.3:
Trends in annual temperature extremes at Majuro (left) and Kwajalein (right). The 95% confidence intervals are shown in parentheses, and trends significant at the 95% level are shown in bold. Hot and cool days, and warm and cold nights are measured relative to 1961–1990 (see Chapter 1 for details).

	Majuro	Kwajalein
	1956–2020	1951–2020
Number of hot days (days/decade)	+4.70 (-3.40, +14.52)	+6.13 (-2.11, +13.81)
Number of warm nights (nights/decade)	**+13.48** (+4.41, +20.39)	**+14.96** (+8.96, +20.40)
Number of cool days (days/decade)	**-1.08** (-6.62, +4.03)	**-3.58** (-7.71, 0.32)
Number of cold nights (nights/decade)	**-3.31** (-6.26, 0.85)	**-5.77** (-8.08, 3.92)
Cooling degree days (degree days/decade)	**+32.03** (+7.41, +53.41)	**+41.09** (+25.35, +56.07)
Daily temperature range (°C/decade)	-0.08 (-0.22, +0.05)	-0.06 (-0.18, +0.04)

Figure 6.7:
Annual number of hot days and cold nights at Majuro (left) and Kwajalein (right). Straight lines indicate linear trends. The magnitudes of the trends are presented in Table 6.3. Diamonds indicate years with insufficient data for one or both variables.

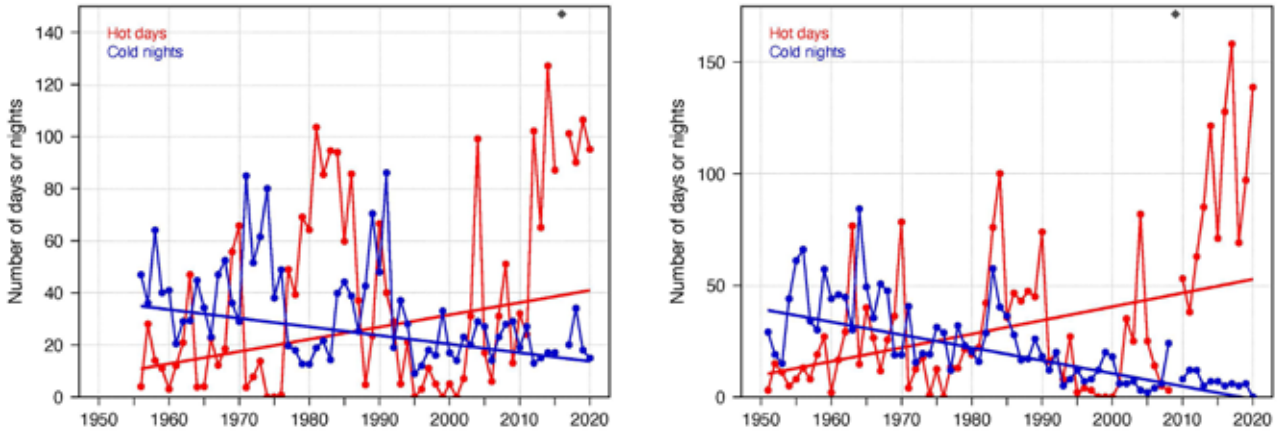

6.6 Tropical cyclones

6.6.1 Seasonal cycle

Tropical cyclones usually affect RMI year-round. The tropical cyclone archive of the western North Pacific indicates that between the 1969 and 2017 seasons, 111 tropical cyclones (Figure 6.8) passed within the EEZ. This represents an average of 23 cyclones per decade.

Tropical cyclones were most frequent in El Niño years (48 cyclones per decade), followed by neutral years (19 cyclones per decade) and least frequent in La Niña years (5 cyclones per decade).

Interannual variability in the number of tropical cyclones in the EEZ is large, ranging from zero in some seasons to 11 in 1972 and 1997 (Figure 6.8). High interannual variability and the small number of tropical cyclones occurring in the EEZ make reliable identification of long-term trends in frequency and intensity difficult.

Some tropical cyclone tracks analysed in this section include the tropical depression stage (sustained winds ≤34 knots) before and/or after tropical cyclone formation.

Figure 6.8:
Number of tropical cyclones passing within the EEZ per season. Each season is defined by the ENSO status, with light blue being an El Niño year, dark blue a La Niña year and grey showing a neutral ENSO year. The 11-year moving average is presented as a purple line and considers all years.

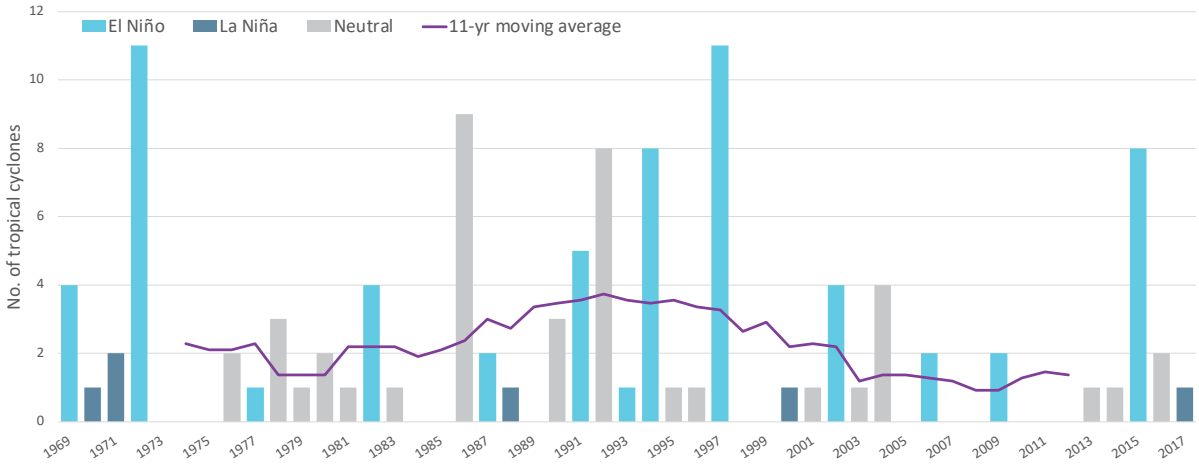

6.6.2 Trends

Trends in total number of tropical cyclones (<995 hPa) and severe tropical cyclones (<970 hPa) are presented for the period 1981–2021 for the Northwest Pacific (125°E–180°W; 0–20°N). Trends are presented at a regional scale as the number of tropical cyclones occurring within Pacific Island EEZs is insufficient for reliable long-term trend analysis.

For the total number of tropical cyclones, the trend (and 95% confidence interval) is -0.56 (-1.84, 0.72) tropical cyclones/decade. There has been little change in the total number of tropical cyclones over the last 41 seasons.

For the total number of severe tropical cyclones, the trend is -0.15 (-1.19, 0.89) tropical cyclones/decade. There has been little change in the number of severe tropical cyclones over the last 41 seasons. There has also been little change in the proportion of tropical cyclones reaching severe status. The trend is 0.01 (-0.04, 0.05) tropical cyclones/decade.

Records of tropical cyclones exist from the late 1800s in some countries in the Northwest Pacific, but trends in tropical cyclones have only been presented from 1981/82. Satellite-based observations began in the early 1970s, but consistent coverage and reliable intensity estimates have only been available since the early 1980s. Confidence in tropical cyclone trends is moderate as the definition of a tropical cyclone has changed and satellite observation methods have continued to improve over the last 41 years.

6.7 Sea surface temperature

6.7.1 Seasonal cycle

Ocean temperature, as measured by the Majuro tide-gauge from 1993 to 2021, reaches on average a maximum of 29.5 °C (85.1 °F) in September/October, but individual months can get as high as 31.0 °C (87.8 °F) between August and November (Figure 6.9). Minimum average temperature is 28.0 °C (82.4 °F) in February. Temperatures can be up to 2 °C (3.6 °F) higher or lower than these averages, although 50% of observations fall within 1 °C (1.8 °F) of the average between August and November, and within 0.5 °C (0.9 °F) in the remainder of the year.

Figure 6.9:
Annual temperatures measured at the Majuro tide-gauge. Blue dots show the monthly average, and shaded boxes show the middle 50% of observations. Lines show the top and bottom 25% of observations.

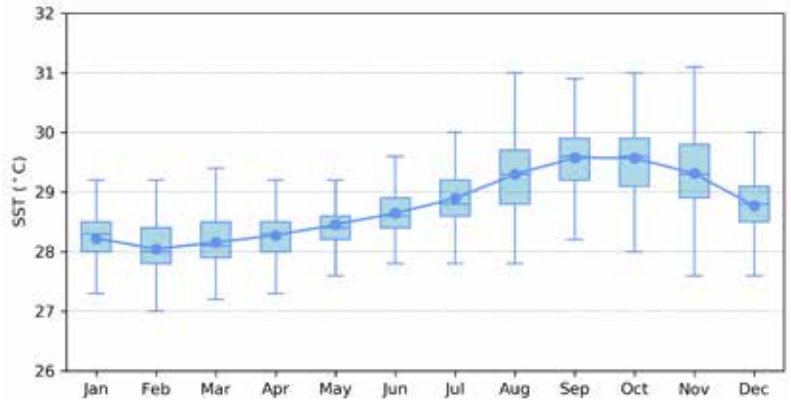

6.7.2 Trends

Figure 6.10 shows the 1981–2021 SST from satellite observations averaged over the EEZ. The data show a trend of 0.25 °C (0.45 °F) per decade with a 95% confidence interval of ±0.05 °C (0.09 °F).

Figure 6.10:
Sea surface temperature from satellite observations averaged across the RMI EEZ, shown as the orange line. The blue line shows the linear regression trend.

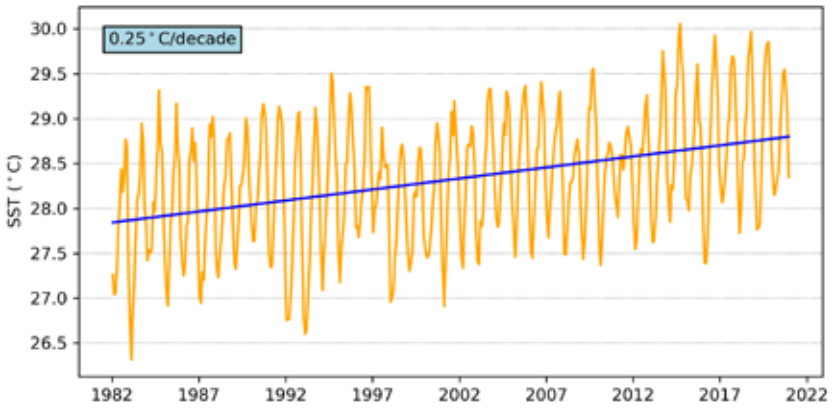

6.8 Sea level

6.8.1 Seasonal cycle

Majuro experiences a semidiurnal tidal cycle, meaning two high and two low tides per day. The highest predicted tides of the year typically occur from February to April as well as August/September. Figure 6.11 shows the number of hours the 99th percentile (2.2 m, 7.2 ft) sea level threshold is exceeded per month across the entire sea level record at Uliga, Majuro. Peak sea levels can occur between September and April but are primarily in February and September/October.

Since approximately 2005, more hours each year exceed the 99th percentile threshold. This is due to a combination of sea-level rise and subsidence occurring at RMI (Brown et al. 2020).

Figure 6.11:
Number of hours exceeding 99th percentile sea level threshold per month from 2001 to 2020 at the Majuro tide-gauge. Blue shading indicates the number of hours, and the final row provides a percentage summary of all the years.

Number of hours exceeding 2.2 m (Uliga, Marshall Islands)

	Jan	Feb	Mar	Apr	May	Jun	Jul	Aug	Sep	Oct	Nov	Dec	Annual
1993	0	0	0	0	0	0	0	0	0	0	0	0	0
1994	0	0	0	0	0	0	0	0	0	0	0	0	0
1995	0	0	0	0	0	0	0	0	0	0	0	0	0
1996	0	0	0	0	0	0	0	0	0	0	0	0	0
1997	0	0	1	0	0	0	0	0	0	0	0	0	1
1998	0	0	0	0	0	0	0	0	0	1	0	0	1
1999	0	0	0	0	0	0	0	0	0	0	0	0	0
2000	0	0	0	0	0	0	0	0	0	0	0	0	0
2001	0	4	0	0	0	0	0	0	0	0	0	0	4
2002	0	0	1	0	0	0	0	0	0	0	0	0	1
2003	0	0	0	1	0	0	0	0	0	0	0	0	1
2004	0	0	0	0	0	0	0	0	0	0	0	0	0
2005	0	0	0	0	0	0	0	0	0	0	0	0	0
2006	2	4	2	0	0	0	0	0	0	0	0	0	8
2007	0	1	0	3	0	0	0	0	10	2	0	0	16
2008	0	0	0	0	0	0	0	0	0	0	0	0	0
2009	0	1	0	0	0	0	0	0	0	0	0	0	1
2010	0	0	2	0	0	0	0	0	3	0	0	0	5
2011	0	8	1	0	0	0	0	0	3	1	0	0	13
2012	0	0	0	3	1	0	0	0	0	0	0	0	4
2013	0	0	0	0	0	0	0	0	0	0	0	0	0
2014	0	3	1	0	0	0	0	0	0	0	0	0	4
2015	0	1	0	0	0	0	0	0	0	0	0	0	1
2016	0	0	4	0	0	0	0	0	9	16	2	0	31
2017	0	0	3	0	0	0	0	0	0	0	6	3	12
2018	7	3	0	0	0	0	0	0	0	0	0	0	10
2019	1	2	1	0	0	0	0	2	13	2	0	0	21
2020	0	6	2	0	0	0	0	0	3	4	1	0	16
2021	0	1	0	0	0	0	0	0	0	12	4	2	19
Monthly Totals (%)	6	20	11	4	1	0	0	1	24	22	8	3	

6.8.2 Trends

Sea level at RMI, measured by satellite altimeters (Figure 6.12) since 1993, has risen between 1 mm (0.04 in) per year in the north and 4.5 mm (0.18 in) per year in the south, which is larger than the global average of 3.1 ± 0.4 mm (0.12 ± 0.02 in) per year (von Schuckmann et al. 2021). The 95% confidence interval ranges from ±0.6 mm (±0.02 in) in central to west regions and up to ±1.0 mm (±0.04 in) in the far west. This rise is partly linked to a pattern related to climate variability from year to year and decade to decade.

Trend estimates at the Majuro tide-gauge over a similar time span to the altimetry observations (May 1993 to July 2020) are provided in the PSLGM Monthly Data Report for July 2020 (http://www.bom.gov.au/ntc/IDO60101/IDO60101.202007.pdf). For Majuro, the trend is reported as 4.7 mm (0.2 in) per year, which is higher than the altimetry trends shown in Figure 6.12 (tide-gauge indicated by star symbol). This difference is most likely attributed to subsidence occurring at Pohnpei (Brown et al. 2020).

Figure 6.12:
Satellite altimetry annual trend for the Pacific from 1993 to 2020, with the RMI EEZ highlighted. The star symbol indicates the location of the tide-gauge at Majuro.

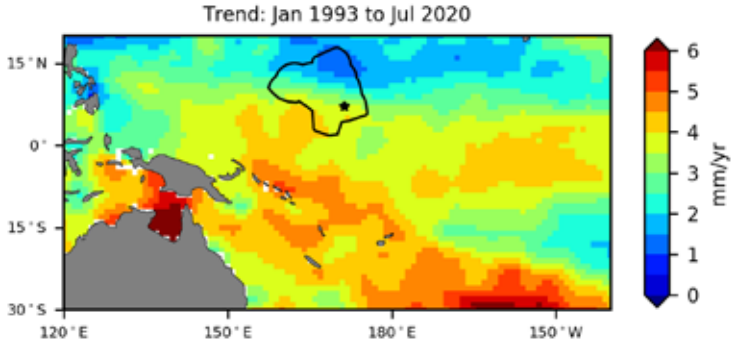

6.9 Waves

6.9.1 Seasonal cycle

The average wave climate in Majuro is defined by the significant wave height, peak period and peak direction. The significant wave height is the mean wave height (from trough to crest) of the highest one third of waves and corresponds to the wave height that would be reported by an experienced observer. Peak period is the time interval between two waves of the dominant wave period. Peak direction is the direction from which the dominant waves are coming.

The average sea state is dominated by wind seas from the northeast. The annual mean wave height is 1.56 m (4.99 ft), the annual mean wave direction is 54° and the annual mean wave period is 9.70 s. In the Pacific, waves often come from multiple directions and for different periods at a time. In Majuro, there are often more than three different wave direction/period components coming from the southeast to southwest (Figure 6.13).

Figure 6.13:
Annual wave rose for Majuro. Note that direction is where the wave is coming from.

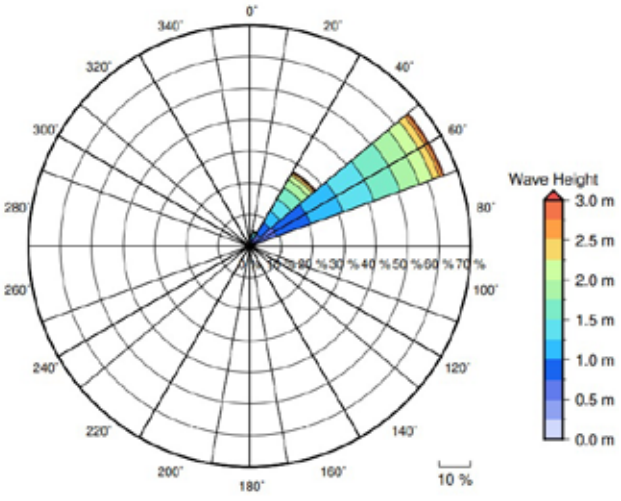

Seasonal wave activity peaks between November and March in terms of both wave height and period (Figure 6.14) due to North Pacific extra-tropical storm activity. Conversely, there is a distinct lull from May to July in terms of wave period and August to October in terms of wave height.

Figure 6.14:
Monthly wave height (black line), wave period (red line) and wave direction (arrows). The grey area represents the range of wave height between calm periods (10% of lowest wave height) and large wave events (10% of highest wave height).

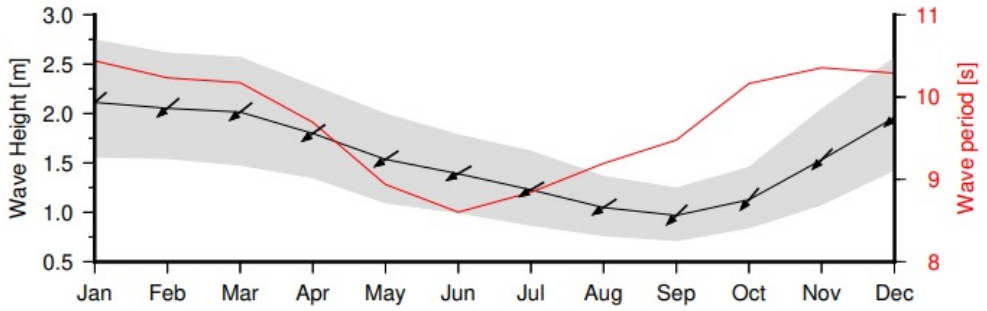

6.9.2 Trends

Waves change from month to month with the seasons, but they also change from year to year with climate oscillations. Typically, these changes are smaller than the seasonal changes but can be important during phenomena such as ENSO. In Majuro, the mean annual wave height has remained unchanged since 1979 (Figure 6.15). The mean annual wave height in Majuro is not significantly correlated with the main climate indicators of the region.

Figure 6.15:
Annual wave height (black line), wave period (red line) and wave direction (arrows). The grey area represents the range of wave height between calm periods (10% of lowest wave height) and large wave events (10% of highest wave height).

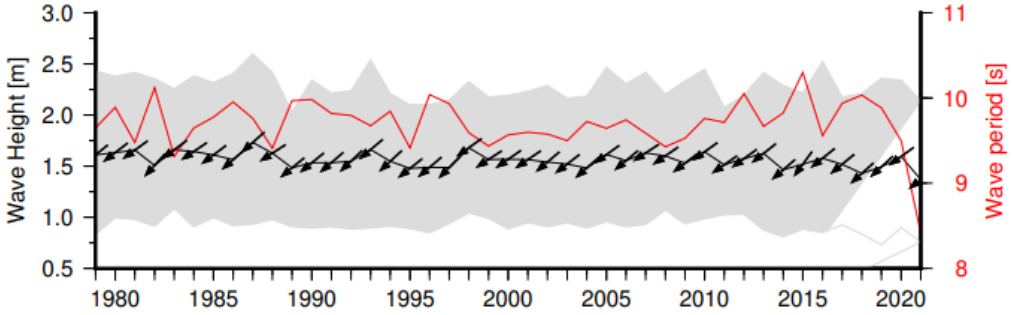

6.9.3 Extreme waves

Extreme wave analysis completed for Majuro was done by defining a severe height threshold and fitting a generalized Pareto distribution (GPD). The optimum threshold selected was 3.09 m (10.14 ft). In the 42-year wave hindcast, 110 wave events reached or exceeded this threshold, averaging 2.6 events per year. The GPD was fitted to the largest wave height reached during each of these events (Figure 6.16, Table 6.15). Extreme wave analysis is a very useful tool but is not always accurate because the analysis is very sensitive to the data available, the type of distribution fitted and the threshold used. For example, this analysis does not accurately account for tropical cyclone waves. More in-depth analysis is required to obtain results appropriate for designing coastal infrastructure and coastal hazard planning.

Figure 6.16:
Extreme wave distribution for Majuro. The crosses represent the wave events that have occurred since 1979. The solid line is the statistical distribution that best fits past wave events. The dashed lines show the upper and lower confidence limits of the fit. There is a 95% chance that the fitted distribution lies between the two dashed lines. Note that the annual return interval is in logarithmic scale.

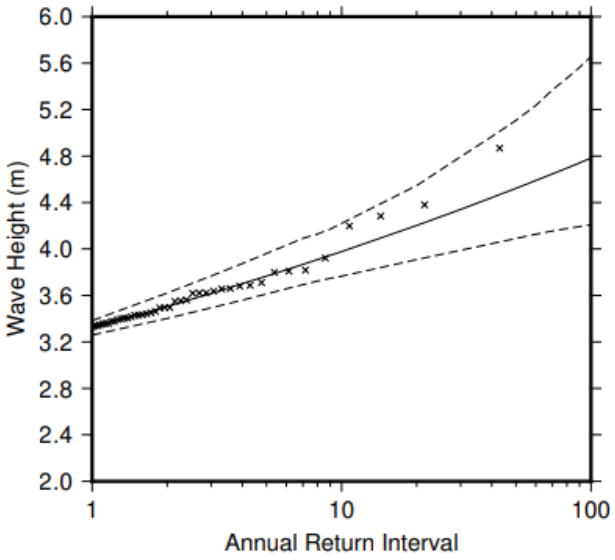

Table 6.4:
Summary of the results from extreme wave analysis in Majuro

Large wave height (90th percentile)	2.29 m (7.51 ft)
Severe wave height (99th percentile)	2.92 m (9.58 ft)
1-year ARI wave height	3.32 m (10.89 ft)
10-year ARI wave height	3.98 m (13.06 ft)
20-year ARI wave height	4.20 m (13.78 ft)
50-year ARI wave height	4.52 m (14.83 ft)
100-year ARI wave height	4.78 m (15.68 ft)